AN OVERVIEW OF THE DUST, CO_2 AND WATER CYCLES ON MARS AS REVEALED FROM IN-SITU ENVIRONMENTAL DATA FROM THE VIKING TO THE CURIOSITY ROVER

G. M. Martínez, Department of Climate and Space Sciences and Engineering, University of Michigan, Ann Arbor, MI, USA *(gemartin@umich.edu)*, **A. De Vicente-Retortillo,** Departamento de Física de la Tierra, Astronomía y Astrofísica II, Universidad Complutense de Madrid, Madrid, Spain, **A. G. Fairén,** Centro de Astrobiología (CSIC-INTA), 28850 Madrid, Spain and Department of Astronomy, Cornell University, Ithaca, NY 14853, USA, **E. Fischer**, Department of Climate and Space Sciences and Engineering, University of Michigan, Ann Arbor, MI, USA, **M. Genzer**, Finnish Meteorological Institute, Erik Palménin aukio 1, Helsinki, Finland, **S. D. Guzewich**, NASA Goddard Space Flight Center, Greenbelt, Maryland, USA, **R. M. Haberle**, Space Science Division, NASA Ames Research Center, Moffett Field, California, USA, **A.-M. Harri**, Finnish Meteorological Institute, Erik Palménin aukio 1, Helsinki, Finland, **O. Kemppinen**, Department of Physics, Kansas State University, Manhattan, Kansas 66506-2601, USA, **M. Lemmon**, Department of Atmospheric Sciences, Texas A&M University, College Station, TX 77843-3150, USA, **C. Newman**, Aeolis Research, 600 N. Rosemead Blvd, Suite 205, Pasadena, CA 91107, USA, **N. Renno**, Department of Climate and Space Sciences and Engineering, University of Michigan, Ann Arbor, MI, USA, **M. Richardson**, Aeolis Research, 600 N. Rosemead Blvd, Suite 205, Pasadena, CA 91107, USA, **M. D. Smith**, NASA Goddard Space Flight Center, Greenbelt, Maryland, USA, **M. Torre-Juárez**, Jet Propulsion Laboratory, California Institute of Technology, 4800 Oak Grove Drive, Pasadena, CA 91109, USA, **A. R. Vasavada**, Jet Propulsion Laboratory, California Institute of Technology, 4800 Oak Grove Drive, Pasadena, CA 91109, USA.

Introduction: The global atmospheric circulation of Mars is mainly regulated by the dust and CO_2 cycles [1], which are triggered by strong seasonal asymmetries in the solar insolation at the top of the atmosphere between the aphelion and perihelion seasons caused by the large eccentricity of Mars' orbit. Dust is ubiquitous in the Martian atmosphere and interacts strongly with solar and thermal radiation, affecting weather and climate and playing a major role on regional and global circulations [2]. In combination with dust transport, the Martian atmospheric circulation is affected strongly by the seasonal deposition of about 30% of the mass of the atmosphere in the polar caps during the cold seasons and its sublimation during the warm seasons [3]. The H_2O cycle is also important because it is related to the stability of water ice deposits and formation of water ice clouds [4].

Here, we present an overview of the complete set of in-situ environmental data obtained from the Viking landers in the 1970s to today's Curiosity rover [5] with focus on the dust, CO_2 and water cycles. In particular, we analyze measurements of atmospheric opacity, atmospheric pressure and near-surface relative humidity to characterize the variability of these quantities at various time scales.

Environmental stations on Mars: In-situ measurements at the surface of Mars have been conducted by the Viking Lander 1 (VL1), Viking Lander 2 (VL2), Mars Pathfinder (MPF) Lander and Sojourner rover, Mars Exploration Rover A (MER-A, Spirit) and B (MER-B, Opportunity), Phoenix lander (PHX) and Mars Science Laboratory (MSL, Curiosity) rover.

Here we focus on in-situ measurements of atmospheric opacity, pressure and near-surface relative humidity conducted by the Viking Meteorology Instrument System (VMIS) and Viking lander camera onboard the VL1 and VL2 landers, the Atmospheric Structure Instrument/Meteorology (ASIMET) package and the Imager for Mars Pathfinder (IMP) onboard the MPF lander, the Pancam instruments onboard the MER rovers, the Meteorological Station (MET) and Phoenix Surface Stereo Imager (SSI) onboard the PHX lander and the Rover Environmental Monitoring Station (REMS) and Mastcam instrument onboard the Curiosity rover.

Results: Next we show the seasonal and interannual variability of atmospheric opacity, near-surface atmospheric pressure and relative humidity using measurements of the highest confidence possible obtained from the Viking landers to the Curiosity rover [5].

Atmospheric Opacity: Fig. 1 shows the seasonal and interannual variability of the atmospheric opacity observed at the VL1, VL2, MPF, MER-A, MER-B, PHX and MSL landing sites as a function of solar longitude. We use measurements taken at 670 nm by the VL cameras, 883 nm by the MPF/IMP, 880 nm by the MER/Pancam cameras, 887 nm by the PHX/SSI and 880 nm by the MSL/Mastcam. During the aphelion season ($L_s = 0° − 180°$), atmospheric opacity values are comparatively low and the intraseasonal and interannual variability is small at each landing site. In contrast, during the perihelion season ($L_s = 180° − 360°$) the opacity values and the intraseasonal and interannual variability are larger, regardless the hemispheric location.

Repeated regional dust storms during the perihelion season between $L_s = 210°$ and $240°$ and between
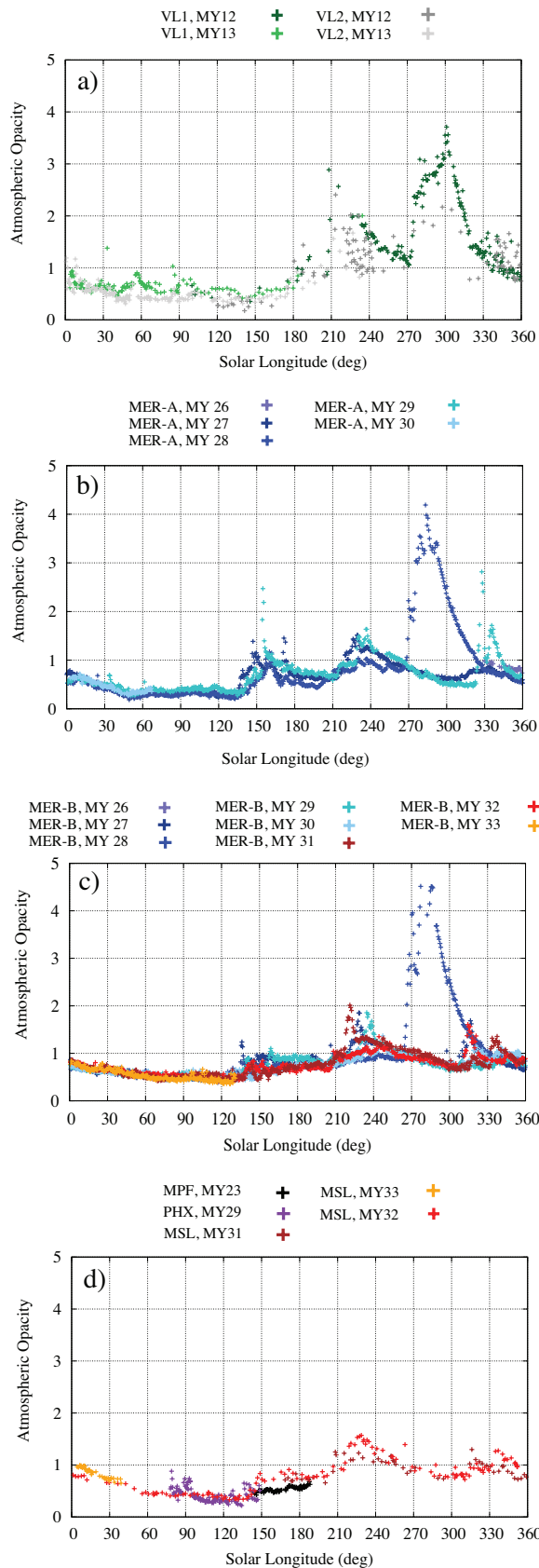
Figure 1. *Interannual and seasonal evolution of the atmospheric opacity at the VLs (a), MER-A (b), MER-B (c) and MPF, PHX and MSL (d) landing sites for each Martian year.*

$L_s = 320°$ and $340°$ produce seasonal increases in the atmospheric opacity at each landing site every year (Fig. 1), while sporadic global dust storms between $L_s = 280°$ and $300°$ produce larger increases in atmospheric opacity every few years (see MY12 and MY28 in Figs. 1a-c). During global dust storms, dust opacity values rapidly increase by a factor of up to four and the surface environmental conditions are significantly altered, with dramatic increases in the diurnal amplitude of the surface pressure and decreases in the diurnal amplitude of the near-surface air temperature. However, values of the daily mean near-surface air temperature are not significantly changed because colder daytime temperatures are counterbalanced by warmer nighttime temperatures [5].

A global dust storm has not occurred during the first two Martian years of the MSL mission (Fig. 1d). The MPF and PHX missions did not observe any global dust storms because they were short and ended prior to the beginning of the dusty season ($L_s = 188°$ and $148°$, respectively).

Atmospheric Pressure: Fig. 2 shows the daily mean atmospheric surface pressure measured during the VL1, VL2, MPF, PHX, and MSL missions as a function of solar longitude.
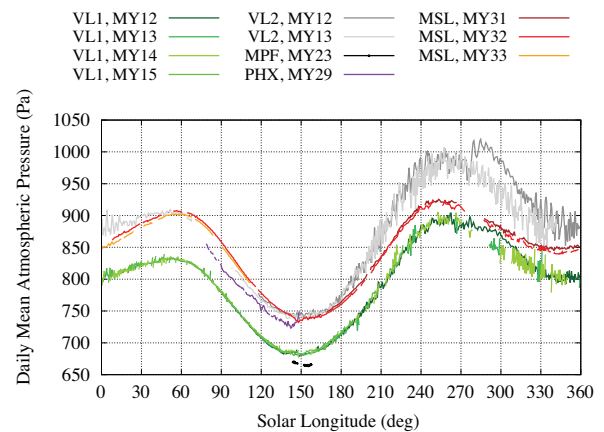
Figure 2. *Interannual and seasonal evolution of the daily mean atmospheric pressure at the VL1 (green colors), VL2 (gray colors), MPF (black), PHX (purple) and MSL (brown-red-orange) landing sites for each Martian year.*

At each landing site, the surface pressure shows an absolute annual maximum at $L_s \sim 260°$ (sublimation of the southern polar cap) and an absolute annual minimum at $L_s \sim 150°$ (condensation onto the southern polar cap). The annual amplitude of the surface pressure increases with increasing latitude. The relative minimum in late southern summer ($L_s \sim 345°$) and relative maximum in late southern fall ($L_s \sim 55°$) at each landing site are caused by the deposition and sublimation of CO_2 into and from the northern polar cap.

The interannual variability is extremely small at the VL sites, with the exception of the major increase in the pressure at the VL2 site (and to a lesser degree at the VL1 site) during the northern winter ($L_s \sim 280°$) in MY12 (Fig. 2). This pressure increase was caused by a global dust storm (Fig. 1a) [6]. The interannual variability at the MSL landing site is also weak (Fig. 2), although a small decrease in the mean surface pressure is observed over the years. This small annual pressure decrease (~8-10 Pa) is mostly accounted for by the change in altitude as the Curiosity rover has been moving uphill, climbing ~100 m (from -4520 to -4420 m) since the beginning of the operations at the surface of Mars.

The sol-to-sol variability at each landing site is relatively small during the aphelion season, increasing significantly during the perihelion season particularly at the VL2 site (Fig. 2). The larger sol-to-sol variations during the perihelion season are caused by baroclinic instability during northern autumn and winter, which strengthens towards the latitude of the polar jet stream [7]. At the MSL site in the southern-hemispheric [8], sol-to-sol variations are also larger during northern autumn and winter. This is caused by strong inter-hemispheric asymmetry in transient eddy activity forced by topography [7], with low-pressure cyclones occurring more often in northern high latitudes during northern autumn and winter than in southern high latitudes during southern autumn and winter.

Near-surface relative humidity: Of all the missions landed on Mars, only the PHX and MSL carried sensors to measure the near-surface relative humidity [9].

Among the full set of REMS RH measurements, only those taken during the first four seconds of measurements after the RH sensor has been turned on after ~5 min of inactivity are reliable. This is because heating of the sensor by the REMS control electronics causes an artificial decrease in the RH values after the first four seconds of operations. Fig. 3 shows an example of the RH sensor measuring strategy on sol 1137.

Using REMS RH measurements selected as described above and obtained with the latest recalibration parameters (August, 2016), we show in Fig. 4 the interannual and seasonal variability of the daily maximum RH value during the first 1258 sols of the MSL mission, along with corresponding values of the volume mixing ratio (VMR) derived from simultaneous REMS measurements of temperature and pressure as $VMR = RH \times e_s(T)/P$, where e_s is the saturation vapor pressure over ice.

The strong seasonal variability of the daily maximum RH (Fig. 4, top) is mainly controlled by near-surface temperatures and not by atmospheric water content. The highest annual values of about 70% occur in early winter ($L_s = 93°$), coinciding with the minimum annual near-surface air temperatures,

while the lowest annual (daily maximum) RH values of ~10% occur around late spring and early summer, coinciding with the highest annual near-surface air temperatures [10].
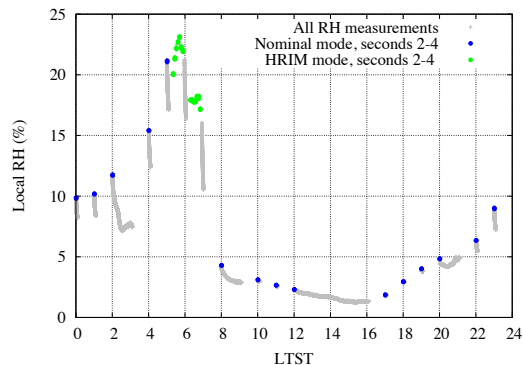
Figure. 3. *Example of MSL/REMS RH sensor measurement strategy on sol 1137. The complete set of RH measurements is shown in gray. Blue circles represent measurements obtained in the nominal mode (first five minutes of every hour) but only during seconds 2, 3 and 4 after the RH sensor has been turned on after ~5 min of inactivity. Green circles represent measurements obtained during seconds 2, 3 and 4 in the so-called high-resolution interval mode (HRIM), which consists of alternately switching on and off the sensor at periodic intervals to minimize heating.*
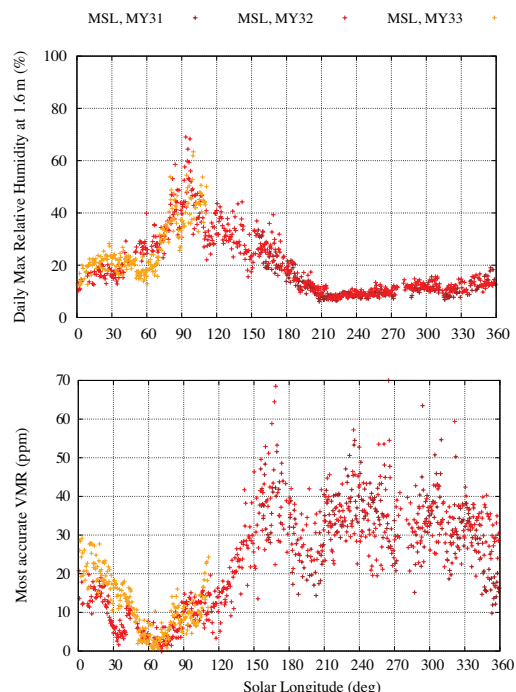
Figure 4. *(Top) Daily maximum RH during the first 1258 sols of the MSL mission. The daily maximum RH is generally achieved between 4 and 6 am. (Bottom) Most accurate VMR value per sol at the MSL landing site obtained at the same time as the RH shown above.*

The seasonal evolution of the daily maximum RH is anti-correlated with that of the near-surface VMR shown in Fig. 4 (bottom). The lowest annual values of VMR occur in late fall and winter, when the daily maximum RH is the highest, while the highest annual values of VMR occur in late winter, spring and early summer, when the daily maximum RH is the lowest.

Surface frost: The detection of surface frost is important because it allows for an independent estimation of water vapor content provided that the temperature is measured. In addition, surface frost formation provides clues to quantify the exchange of water vapor between the regolith and the atmosphere on Mars [11,12].

At the PHX site, nighttime frost was detected by the Robotic Arm Camera from sol 80 (early summer, L_s = 113°) until the end of the mission on sol 151 (late summer, L_s =149°) [13]. Moreover, not only the ground was saturated at the PHX landing site but also the near-surface atmosphere, where nighttime temperatures are higher than at the ground due to strong thermal inversions [12,14,15]. Considering typical nighttime temperatures of about 195 K at the PHX landing site, an estimate for the near-surface nighttime water vapor VMR of about 100 ppm is obtained. Such an estimate is higher than the annual maximum values at the MSL site (Fig. 4, bottom) and is in agreement with satellite estimations of the column water content showing greater values at the PHX site [10].

At the Viking Lander 2 site, a thin layer of frost was observed on the ground for about 250 sols, from late fall (L_s = 230°) until early spring (L_s = 16°) in the first year of the mission [16]. At this location, surface frost formed at night and persisted throughout the day, whereas at lower latitudes such as those of VL1, MPF, MER and MSL missions, ground frost events have not been observed by landers or rovers.

Discussion: The characterization of dust-lifting processes is of paramount importance for shedding light on the dust cycle [17,18]. However, these processes are poorly understood because of the lack of measurements. Only the Dust Characterisation, Risk Assessment and Environment Analyser on the Martian Surface (DREAMS) instrument onboard the ExoMars 2016 lander will provide new insight into dust lifting by measuring electric forces. Measurements of the various components of the dust cycle, including atmospheric opacity, saltation, and the surface heat budget in combination with regolith wetness can shed light on dust-lifting processes.

The exchange of water vapor between the regolith and the atmosphere at different time scales is important to understand the water cycle on Mars [12]. Using MSL/REMS RH measurements, values of the near-surface water vapor content can only be accurately derived at nighttime when RH values are sufficiently high and thus the resulting uncertainty in VMR is low [10,11]. Therefore, measurements of near-surface water vapor content throughout the diurnal cycle and of vertical turbulent fluxes of water vapor between the surface and the atmosphere are important to shed light on the H_2O cycle.

Bibliography: [1] Read, P. L. and S. R. Lewis (2004)*, The Martian Climate Revisited: Atmosphere and Environment of a Desert Planet, Springer,* Chichester, U. K. [2] Kahre, M. A. et al. (2006), Modeling the Martian dust cycle and surface dust reservoirs with the NASA Ames general circulation model, *J. Geophys. Res., 111*, E06008. [3] Hess, S. L. et al. (1980), The annual cycle of pressure on Mars measured by Viking landers 1 and 2, *Geophys. Res. Lett., 7*(3), pp.197-200. [4] Madeleine, J. B. et al. (2012), The influence of radiatively active water ice clouds on the Martian climate, *Geophys. Res. Lett., 39*(23). [5] Martínez, G. M. et al. (2016), Characterization of the Martian Climate near the surface: A review of in-situ data from Viking to Curiosity, *Space Sci. Rev.* (submitted). [6] Fenton, L. K. and M. I. Richardson (2001), Martian surface winds- Insensitivity to orbital changes and implications for aeolian processes, *J. Geophys. Res, 106*, p.32. [7] Barnes, J. R. (1981), Midlatitude disturbances in the Martian atmosphere: A second Mars year, *J. Atmos. Sci., 38*(2), 225-234. [8] Harri, A.-M., et al. (2014), Pressure observations by the Curiosity rover: Initial results, *J. Geophys. Res.: Planets* 119.1: 82-92. [9] A.-M. Harri, et al. (2014), Mars Science Laboratory relative humidity observations: Initial results, *J. Geophys. Res.: Planets, 119*(9), pp.2132-2147. [10] Martínez, G. M. et al. (2015), Likely frost events at Gale crater: Analysis from MSL/REMS measurements, *Icarus.* [11] Savijärvi, H. et al. (2016), The diurnal water cycle at Curiosity: Role of exchange with the regolith. *Icarus, 265*, pp.63-69. [12]. Savijärvi, H. and A. Määttänen (2010), Boundary-layer simulations for the Mars Phoenix lander site, *Q. J. Roy. Meteor. Soc., 136*(651), pp.1497-1505. [13] Smith, P. H. et al. (2009), H2O at the Phoenix landing site, *Science 325*, 58-61. [14] Whiteway, J. A. *et al.* (2009), Mars water-ice clouds and precipitation, *Science 325*, 68-70. [15] Zent, A. P. et al. (2016), A revised calibration function and results for the Phoenix mission TECP relative humidity sensor, *J. Geophys. Res. Planets, 121*, 626–651. [16] Wall, S.D. (1981), Analysis of condensates formed at the Viking 2 Lander site: The first winter, *Icarus 47* (2), 173–183. [17] Kok, J.F, and N.O. Renno (2009), A comprehensive numerical model of 400 steady state saltation (COMSALT), *J. Geophys. Res. 114*, D17204. [18] Esposito, F., R. et al. (2016), The role of the atmospheric electric field in the dust-lifting process, *J. Geophys. Res.*